Title
Targeting Wee1 for the treatment of pediatric high-grade gliomas

Journal
Neuro-Oncology, 16(3)

ISSN
1522-8517

Authors
Mueller, Sabine
Hashizume, Rintaro
Yang, Xiaodong
et al.

Publication Date
2014-03-01

DOI
10.1093/neuonc/not220

Peer reviewed

Neuro-Oncology Advance Access published December 4, 2013

Neuro-Oncology

Neuro-Oncology 2013; **0**, 1–9, doi:10.1093/neuonc/not220

Targeting Wee1 for the treatment of pediatric high-grade gliomas

Sabine Mueller, Rintaro Hashizume, Xiaodong Yang, Ilan Kolkowitz, Aleksandra K. Olow, Joanna Phillips, Ivan Smirnov, Maxwell W. Tom, Michael D. Prados, C. David James, Mitchel S. Berger, Nalin Gupta, and Daphne A. Haas-Kogan

Department of Neurology, University of California, San Francisco, San Francisco, California (S.M., I.K.); Department of Pediatrics, University of California, San Francisco, San Francisco, California (S.M., M.D.P., N.G.); Brain Tumor Research Center, University of California, San Francisco Helen Diller Family Comprehensive Cancer Center, San Francisco, California (S.M., R.H., X.Y., A.K.O., J.P., M.W.T., C.D.J., M.S.B., N.G., D.A.H.-K.); Department of Neurological Surgery, University of California, San Francisco, San Francisco, California (S.M., J.P., I.S., M.D.P., C.D.J., M.S.B., N.G., D.A.H.-K.); Department of Radiation Oncology, University of California, San Francisco, San Francisco, California (D.A.H.-K.)

Corresponding author: Sabine Mueller, MD, PhD, Departments of Neurology, Pediatrics, and Neurosurgery, University of California, San Francisco, Helen Diller Cancer Center, 1450 3rd Street San Francisco, CA 94143-0106 (muellers@neuropeds.ucsf.edu).

Background. We investigated the efficacy of the Wee1 inhibitor MK-1775 in combination with radiation for the treatment of pediatric high-grade gliomas (HGGs), including diffuse intrinsic pontine gliomas (DIPGs).

Methods. Gene expression analysis was performed for 38 primary pediatric gliomas (3 grade I, 10 grade II, 11 grade III, 14 grade IV) and 8 normal brain samples using the Agilent 4 × 44 K array. Clonogenic survival assays were carried out in pediatric and adult HGG cell lines ($n = 6$) to assess radiosensitizing effects of MK-1775. DNA repair capacity was evaluated by measuring protein levels of γ-H2AX, a marker of double strand DNA breaks. In vivo activity of MK-1775 with radiation was assessed in 2 distinct orthotopic engraftment models of pediatric HGG, including 1 derived from a genetically engineered mouse carrying a $BRAF^{V600E}$ mutation, and 1 xenograft model in which tumor cells were derived from a patient's DIPG.

Results. Wee1 is overexpressed in pediatric HGGs, with increasing expression positively correlated with malignancy ($P = .007$ for grade III + IV vs I + II) and markedly high expression in DIPG. Combination treatment of MK-1775 and radiation reduced clonogenic survival and increased expression of γ-H2AX to a greater extent than achieved by radiation alone. Finally, combined MK-1775 and radiation conferred greater survival benefit to mice bearing engrafted, orthotopic HGG and DIPG tumors, compared with treatment with radiation alone ($BRAF^{V600E}$ model $P = .0061$ and DIPG brainstem model $P = .0163$).

Conclusion. Our results highlight MK-1775 as a promising new therapeutic agent for use in combination with radiation for the treatment of pediatric HGGs, including DIPG.

Keywords: diffuse intrinsic pontine glioma, MK-1775, pediatric high-grade glioma, radiation, Wee1 inhibition..

High-grade gliomas (HGGs) are aggressive brain tumors in children, with 5-year survival rates <20%. For diffuse intrinsic pontine gliomas (DIPGs), the most common type of glioma arising in the brainstem, the prognosis is even worse, with virtually no long-term survivors.[1] Despite several decades of research efforts, the outcomes for these children have not significantly changed. This lack of progress can be attributed to a lack of understanding of underlying molecular events leading to pediatric HGG and DIPG tumorigenesis and a lack of relevant models for therapeutic drug testing.

A number of genetic and molecular alterations have recently been identified in the oncogenesis of pediatric gliomas. Approximately 15% of pediatric gliomas (World Health Organization grades II–IV) have an activating mutation in the *Braf* gene ($BRAF^{V600E}$). Inhibitors targeting components of this activated pathway are entering clinical trials for the treatment of children with $BRAF^{V600E}$-positive gliomas.[2] Platelet derived growth factor receptor (*PDGFR*) amplification has also been reported in subsets of HGGs and DIPGs, with crenolanib, an inhibitor of PDGFR kinase, currently being tested in children and young adults with the latter type of tumor.[3] In addition, recent investigations have found a specific histone mutation (K27M-H3.3) that is present in most DIPGs, whose occurrence is associated with worse clinical outcome.[4,5] Investigations targeting molecular biology related to this mutation are ongoing. The molecular underpinnings of pediatric HGGs and

Received 22 January 2007; accepted 14 October 2013

DIPGs are distinct from those underlying adult gliomas,[6] and therefore the common practice of extrapolating adult therapies to pediatric tumors is precarious. The development of effective strategies for pediatric patients requires laboratory investigations and preclinical testing in relevant, pediatric-specific models.

A potential specific molecular target is Wee1, which is a critical driver of G_2-M cell cycle progression. Activated Wee1 causes inhibitory phosphorylation of Cdc2, preventing G_2-M cell cycle progression. Inhibition of Wee1 in combination with radiation has been shown to reduce tumor growth in adult models of glioblastoma multiforme (GBM), by promoting premature mitosis in cells with damaged DNA.[7] Wee1 inhibition alone has also been shown to have antitumor activity in sarcoma cells leading to apoptotic death.[8] To date, possible links between Wee1 and known aberrations in pediatric HGG and/or DIPGs such as *PDGFR* amplification or the specific K27M-H3.3 mutation remain poorly understood.

MK-1775 is a selective Wee1 kinase inhibitor and currently the only Wee1 inhibitor to enter early phase 1/2 clinical trials in combination with conventional chemotherapy for adults with advanced solid tumors. In this study, we investigated the expression of Wee1 in pediatric gliomas to evaluate its relevance as a therapeutic target and whether combining MK-1775 with radiation is more effective than radiation alone for the treatment of pediatric gliomas. To our knowledge this is the first investigation that reports on the expression of Wee1 in all grades of pediatric gliomas—including DIPG—and uses relevant pediatric glioma models to assess the effect of MK-1775 in combination with radiation.

Materials and Methods

Cell Lines, Xenografts, and Primary Tumors

U87MG and SF188 were obtained from the Brain Tumor Research Center Tissue Bank at the University of California, San Francisco (UCSF). Correct identities for these cell lines, as well as for cell line KNS-42 (Japan Health Sciences Foundation Health Science Research Resource), SF8628 DIPG primary cell culture, and serially passaged GBM36 xenograft,[9] were determined through DNA analysis by the PowerPlex 16 System (Promega). SF10776 murine glioma cells were established and propagated from $BRAF^{V600E}$, Ink4a-$Arf^{-/-}$ transgenic mice, as previously described.[10] SF8628 and SF10776 cells were transduced with a lentiviral vector containing firefly luciferase as previously described[9] to enable in vivo bioluminescence imaging. Collection and analysis of pediatric brain tumor tissues was in accordance with institutional review board approval.

Clonogenic Survival Assays

For clonogenic survival assays, single-cell suspensions were generated for each cell line and cells were seeded into 6-well tissue culture plates. Cells were allowed to adhere for 16 h, then were treated with varying doses of radiation. Cells were irradiated using a cesium source at a dose rate of 1.97 Gy/min, then exposed to MK-1775 during colony formation. Colonies of >50 cells were used to indicate surviving fractions. Surviving fractions were normalized to the plating efficiency of each cell line, as previously described,[11] with data presented as the mean ± SD of quadruplicate samples per treatment condition. Cell survival measurements were fitted to a linear quadratic mathematical model using GraphPad Prism 5.0 software. The dose enhancement ratio (DER) was calculated at 10% survival. The DER is the ratio of the radiation dose required to achieve 10% cell survival using radiation alone and the radiation dose required to achieve the same biological effect (10% cell survival) using radiation plus MK-1775. A DER value >1 indicates that the addition of the drug is functioning as a radiosensitizer.

Western Blot Analysis

Total protein extracts from cells were prepared using cell lysis buffer (50 mM HEPES [4-(2-hydroxyethyl)-1-piperazine ethanesulfonic acid], pH 7.0; 150 mM NaCl; 10% glycerol; 1% Triton X-100; 0.5% sodium deoxycholate; 1% NP-40 [nonyl phenoxypolyethoxylethanol]; 1.5 mM $MgCl_2$; and 10 mM EDTA) containing a complete protease and phosphatase inhibitor cocktail (Roche Diagnostics). Protein lysates were separated by sodium dodecyl sulfate–polyacrylamide gel electrophoresis and transferred to polyvinylidene difluoride membranes. After exposure to primary antibody, membranes were incubated with goat anti-rabbit IgG horseradish peroxidase–conjugated secondary antibody and visualized by ECL (Amersham Pharmacia). Antibodies specific for γ-H2AX and phosphorylated (p-)Cdc2 were obtained from EMD Millipore, and β-actin antibody was obtained from Cell Signaling Technology.

Gene Expression Analysis

RNA extractions from cell lines or from primary tumor samples were performed using a protocol associated with the Qiagen RNA Isolation kit. Gene expression analysis was performed for 38 pediatric gliomas (3 grade I, 10 grade II, 11 grade III, and 14 grade IV, including 1 DIPG tumor [SF8628], 1 DIPG derived xenograft [SF7761], and 8 normal brain samples using the Agilent 4 × 44 K array [Sandler Center, UCSF]). Sample preparation, labeling, and array hybridizations were performed according to standard protocols from the UCSF Sandler Center Functional Genomics Core Facility and Agilent Technologies (http://www.arrays.ucsf.edu and http://www.agilent.com). Arrays were scanned using the Agilent microarray scanner, and raw signal intensities were extracted with Feature Extraction v10.6 software. The dataset was normalized using the *quantile* normalization method proposed by Bolstad et al.[12] Wee1 expression was additionally examined in published gene expression sets of pediatric DIPGs.[13]

Immunohistochemistry of Tumor Samples

Pediatric gliomas were examined on tissue microarrays and used to assess Wee1 expression by immunohistochemistry (IHC). Hybridizations with Wee1 antibody (Santa Cruz Biotechnology) were performed using an automated IHC tissue staining process (Ventana Medical Systems Benchmark XT) that included antigen retrieval for 90 min in Tris buffer. IHC results were scored by a neuropathologist (J.P.) as follows: 0 for <2% of tumor nuclei positive; 1 for 2%–10% of tumor nuclei positive; 2 for 10%–25% tumor nuclei positive; 3 for 25%–75% tumor nuclei positive; 4 for >75% tumor nuclei positive. Digital images were captured with a microscope (Olympus model BX41TF) outfitted with a digital microscope camera (Olympus model DP70).

For IHC analyses of xenografts, tumors were harvested 24 h after the last treatment, fixed in 4% formalin overnight, and processed through ethanol dehydration series prior to paraffin embedding. Five micrometers of paraffin sections were cut, deparaffinized, rehydrated with decreasing ethanol concentrations, and hybridized using anti–γ-H2AX (Cell Signaling), anti–Ki-67 (Dako), or anti–p-Cdc2 (R&D Systems), then detected with diaminobenzidine substrate (Vector Labs). Image-based quantification was performed for each stain. Ten 20× pictures were taken per tumor (Leica DMLS microscope), with positively stained cells quantified. Percentages of positive cells were averaged per tumor, with averages used to assess differences between treatment groups, by both Kruskal–Wallis and Wilcoxon rank sum tests for pairwise comparison. The Goodman–Kruskal gamma statistic was used to analyze IHC scores according to tumor grade.

Cell Cycle Analysis

Cell cycle distributions were determined using flow cytometry following staining with bromodeoxyuridine and 7-amino-actinomycin D. Cells were grown exponentially and treated with MK-1775, followed immediately by

radiation; they were then fixed and stained according to instructions associated with the BD Pharmingen FITC BrdU Flow Kit 24 h after treatment. Fluorescence was measured on a fluorescence activated cell sorting (FACS) flow cytometer (Becton Dickinson), and data were analyzed using FlowJo software (TreeStar).

Gamma-H2AX Cytometric Analysis

Gamma (γ)-H2AX levels were determined using flow cytometry following staining with anti–phospho-histone H2AX fluorescein isothiocyanate conjugate (Millipore). Adherent cells were treated with 200 nM MK-1775 followed immediately by 4 Gy of radiation. At 1, 3, 6, and 24 h after treatment with MK-1775 and radiation, the cells were fixed with 4% paraformaldehyde and permeabilized with ice-cold 90% methanol, then stored in methanol at −20°C when necessary. Fluorescein isothiocyanate fluorescence was measured on a FACS flow cytometer, and data were analyzed using Flow Jo Software (TreeStart).

Animals and Surgical Procedures

The UCSF Institutional Animal Care and Use Committee approved all animal protocols. Five-week-old female athymic mice (nu/nu genotype, Bagg albino/c background) were purchased from Simonsen Laboratories, and animals were housed under aseptic conditions. Luciferase-modified tumor cells were implanted into the brains of athymic mice as previously described.[10,14] Briefly, mice were anesthetized by intraperitoneal injection of 100 mg/kg ketamine and 10 mg/kg xylazine in 0.9% saline. The skulls of the mice were exposed and a small opening made using a 25-gauge needle at 1.5 mm to the right of midline, posterior to the lambdoid suture for injection into the pontine tagmentum, or at 3.0 mm to the right of the midline, just behind the bregma, for tumor cell injection into the caudate putamen. A total of 1.0×10^5 SF8628 cells, in a volume of 1 μL, were injected into the pontine tagmentum (5.0 mm depth from the inner table of the skull), or 3.0×10^5 SF10776 cells, in a volume of 3 μL, were injected into the caudate putamen (3.0 mm depth from the inner table of the skull).

In vivo Bioluminescence Monitoring

To monitor tumor growth in vivo, bioluminescence imaging was performed with the Xenogen IVIS Lumina System using Living Image software for data acquisition (Xenogen). Mice were anesthetized with 100 mg/kg ketamine and 10 mg/kg xylazine and imaged 12 min after i.p. injection of luciferin (D-luciferin potassium salt, 150 mg/kg; Gold Biotechnology). Signal intensity was quantified within a region of interest over the skull, as defined by the Living Image software.

In vivo Treatment of Tumor-bearing Athymic Mice With MK-1775 and Radiation

Athymic mice implanted with luciferase-modified tumor cells were randomized to one of the following treatment groups: vehicle control (Ora-Plus, Paddock Laboratories), radiation (^{137}Cs source, Mark I, model 68A irradiator, JL Shepherd & Associates), MK-1775, or radiation + MK-1775. Tumor-bearing mice were treated with 60 mg/kg MK-1775 twice daily by oral administration for 10 days and/or radiation at 0.5 Gy per day every other day (Mon-Wed-Fri), for a total dose of 3.0 Gy. Mice in the drug-only group received the same amount of MK-1775 compared with mice in the combination group. Radiation was administered between doses of MK-1775 (in the combined modality arm) or Ora-Plus (in the radiation alone arm). Treatments were initiated when intracerebral tumors entered log-phase growth, as indicated by tumor bioluminescence monitoring, which constituted day 9 for SF10776 and day 13 for SF8628. All mice were examined daily for development of symptoms related to tumor growth and twice weekly by bioluminescence imaging as outlined previously.[14,15] Mice were euthanized when they exhibited symptoms indicative of significant impairment of neurological function. In addition to the mice used for therapy survival benefit, mice from each cohort were sacrificed 2 h after completion of the treatment, with brains resected and placed in 4% paraformaldehyde, then processed for IHC analysis.

The Kaplan–Meier estimator was used to generate survival curves, and differences between survival curves were calculated using a log-rank test. Differences between bioluminescence growth curves were compared by a 2-tailed unpaired *t*-test using GraphPad Prism software.

Results

Array Analysis of Wee1 Expression in Pediatric Gliomas

Array-based gene expression analyses of Wee1 in pediatric gliomas revealed that Wee1 was overexpressed in pediatric HGGs relative to normal brain and that extent of overexpression positively correlated with increasing malignancy (grades III and IV compared with grades I and II; 2-sided Student's *t*-test, $P = .007054$; Fig. 1A). Two DIPG cell sources—1 modified for expression of

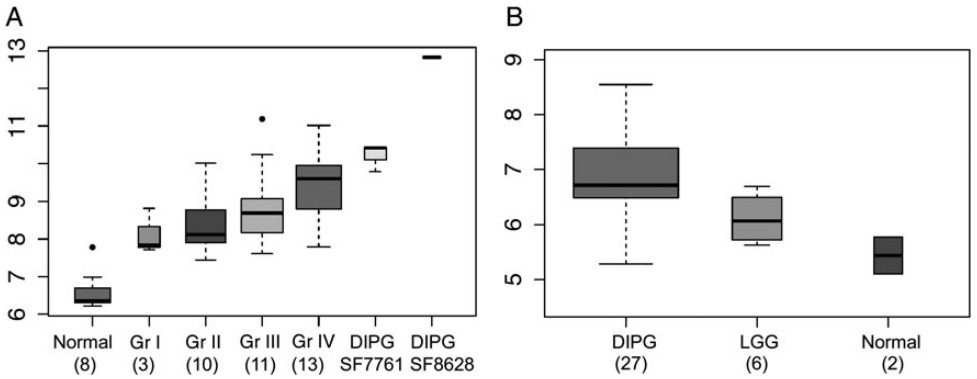

Fig. 1. Elevated Wee1 expression in DIPGs and pediatric HGGs. (A) Box plot showing mean + SD of Wee1 expression in different malignancy grades of tumor. Normal: normal brain; grade (Gr) I ($n = 3$), grade II ($n = 10$), grade III ($n = 11$) and grade IV ($n = 13$). SF7761 is a human telomerase reverse transcriptase immortalized DIPG cell line. SF8628 is a human DIPG surgical specimen. Wee1 expression is significantly greater in HGGs (grades III and IV) than in low-grade gliomas (LGGs; grades I and II) (2-sided Student's *t*-test, $P = .0071$). (B) Wee1 expression in a published expression dataset of pediatric DIPGs ($n = 27$), LGGs ($n = 6$) and normal brain (normal; $n = 2$). Wee1 expression is significantly higher in DIPGs (2-sided Student's *t*-test: $P = .005$ compared with LGGs). *Y*-scale is a log2 transformation of expression measure, and each unit corresponds to a 2-fold change in expression.

human telomerase (SF7761)[14] and 1 established directly from DIPG biopsy (SF8628) without modification—showed particularly high *Wee1* expression. Expression analysis of *Wee1* in a published dataset of DIPGs[13] revealed significant upregulation of Wee1 in DIPGs compared with low-grade gliomas and normal brain (2-sided Student's *t*-test, $P = .0071$; Fig. 1B).

Immunohistochemical Analysis of Wee1

To further examine Wee1 protein expression in pediatric gliomas, we performed IHC analyses of Wee1 in all grades of tumor (grade I, $n = 18$; grade II, $n = 5$; grade III, $n = 7$; grade IV, $n = 13$). Our results show (Fig. 2) greater Wee1 expression in higher-grade tumors (see Supplemental Table S1) and statistically significant correlation with the array analysis (Spearman's rho, 0.49; $P = .033$). Further analysis revealed a positive correlation between IHC scores and tumor grade (Goodman–Kruskal gamma statistic $P = .03$; 2-sided gamma-knife gamma = 0.55).

Antiproliferative Effects of MK-1775 in Combination With Radiation

Clonogenic survival assays, for preliminary investigation of MK-1775 as a radiation sensitizer, were carried out using 6 different glioma cell lines (4 pediatric and 2 adult HGG cell lines). We first examined the timing of MK-1775 administration in relation to radiation therapy by testing simultaneous as well as sequential administration of MK-1775, in relation to radiation treatment, with

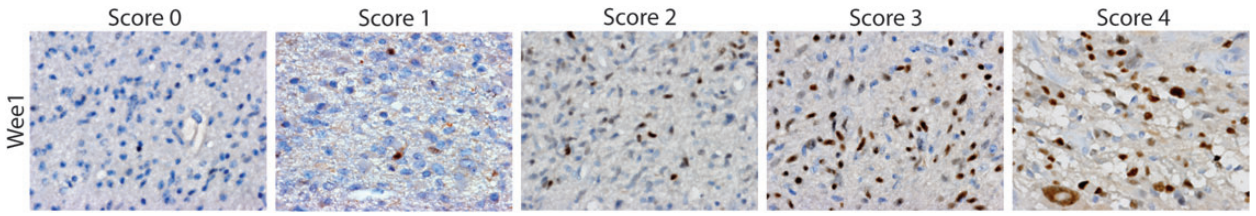

Fig. 2. IHC staining for Wee1 in pediatric HGG. Images show representative results for IHC 0–4 positivity scoring (0, 2, and 3 are grade III tumors; 1 and 4 are grade IV tumors). Magnification, 400×.

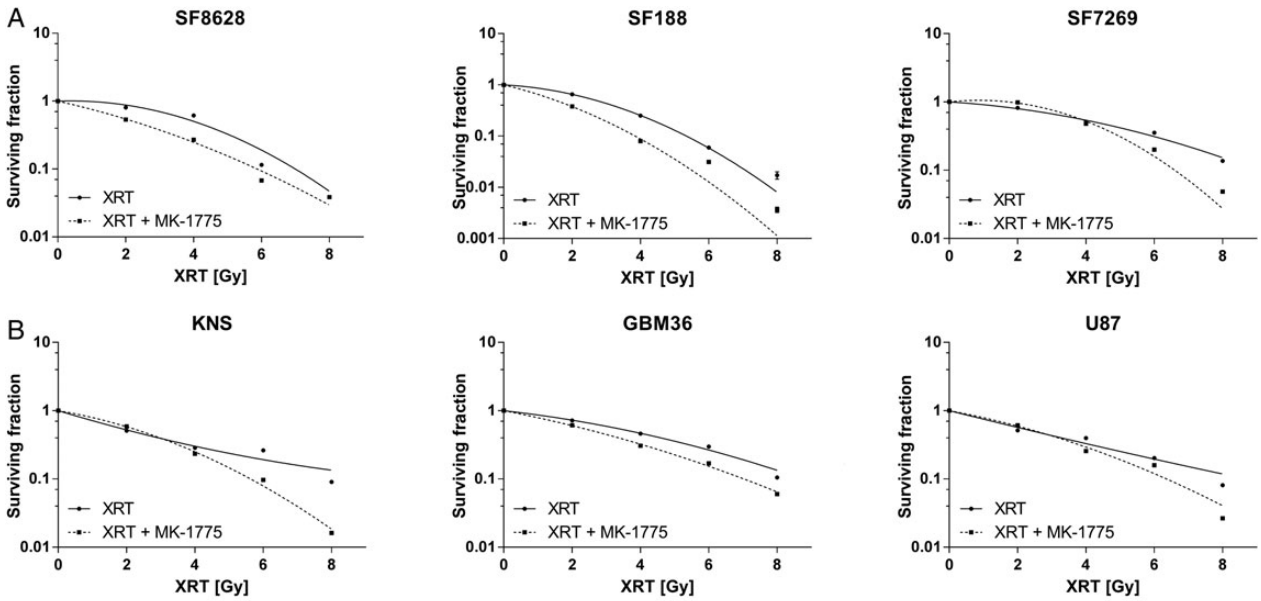

	SF8628 (p53 mt)	SF188 (p53 mt)	SF7269 (p53 wt)	KNS (p53 wt)	GBM36 (p53 mt)	U87 (p53 wt)
DER 10% Survival	1.19	1.39	1.37	1.85	1.25	1.37

Fig. 3. Clonogenic survival results for pediatric and adult glioma cell lines treated with radiation ± MK-1775. (A) Radiation alone: solid line. Radiation + MK-1775: dashed line. MK-1775 (200 nM) was administered 24 h after radiation (0, 2, 4, 6 Gy). Surviving fractions, shown as mean + SE (quadruplicate samples), were normalized to plating efficiency for each cell line. XRT, radiation therapy. Clonogenic survival data points were fitted to a linear quadratic mathematical model. (B) Dose Enhancement Ratio (DER) for each cell line calculated at 10% survival levels. mt, mutant; wt, wild type.

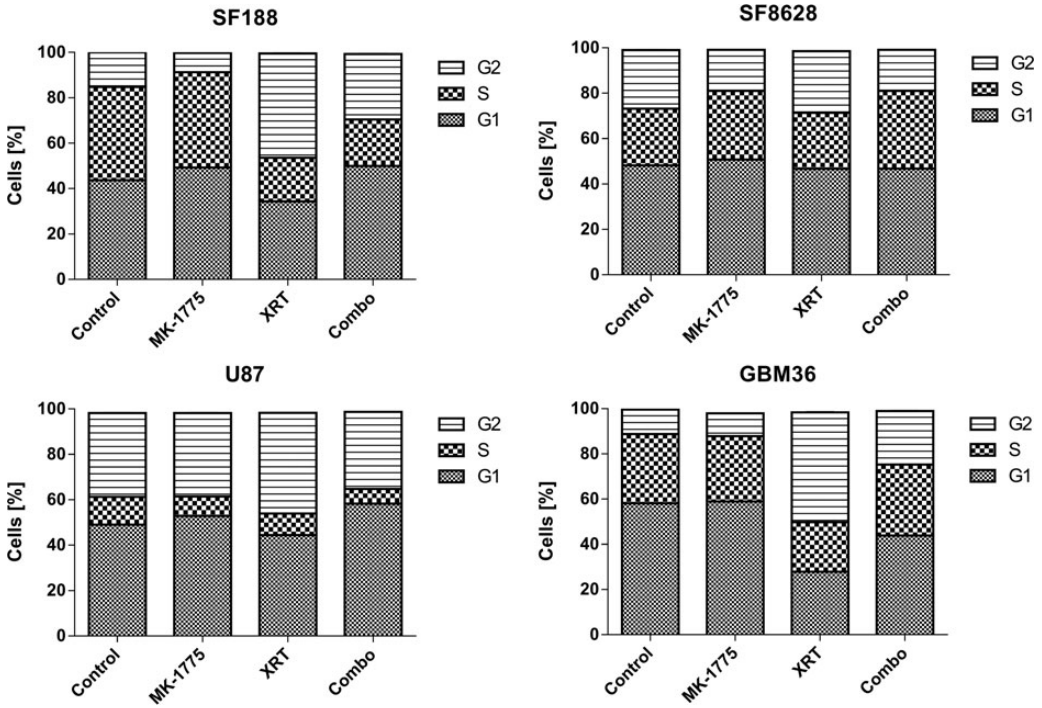

Fig. 4. MK-1775 decreases radiation-induced G_2 cell cycle arrest. Bar graphs display distribution of cells within each cell cycle phase for 4 independent HGG cell lines treated with either radiation therapy (XRT; 4 Gy), MK-1775 (200 nM), MK-1775 + radiation (combo; 200 nM MK-1775 followed immediately by 4 Gy radiation), or control. Cell cycle analyses were performed 24 h after treatment.

MK-1775 administered 3, 6, and 24 h before as well as after radiation. The most pronounced effects were observed for MK-1775 treatment at 24 h after radiation therapy (data not shown), and this sequence of treatment was used for all subsequent clonogenic assays. Figure 3A shows the effect of MK-1775 and radiation therapy on clonogenic survival in these 6 cell lines. Figure 3B shows the DERs for each cell line calculated at the 10% survival level. No consistent differences were noted in DERs based on p53 mutational status.

MK-1775 Abrogates Radiation-induced G_2 Arrest in Pediatric High-grade Gliomas

Based on the mechanism of action of Wee1 and the effects of its inhibitor MK-1775, we hypothesized that combining MK-1775 with radiation would abrogate radiation-induced G_2 arrest. Indeed, our results confirm that in the pediatric glioma cell lines SF188 and SF8628 and in the adult glioma cell lines U87 and GBM36, radiation produces a G_2 arrest that is abrogated by Wee1 inhibitor treatment. MK-1775 alone had minimal to no effect on cell cycle distribution (Fig. 4).

Because G_2 arrest allows repair of DNA damage after irradiation, we anticipated that combining MK-1775 with radiation would increase levels of phosphorylated H2AX (γ-H2AX), a marker of double strand (ds)DNA breaks, since tumor cells with damaged DNA would be less able to undergo cell cycle arrest to repair damaged DNA. As expected, for the pediatric DIPG xenograft SF8628, a combination of MK-1775 and radiation increased levels of γ-H2AX to a greater extent and for longer duration than radiation alone (Fig. 5). Similar effects were observed using flow cytometric analysis in the pediatric glioma cell line KNS-42 and the adult glioma xenograft GBM36 (Supplemental Fig. S1).

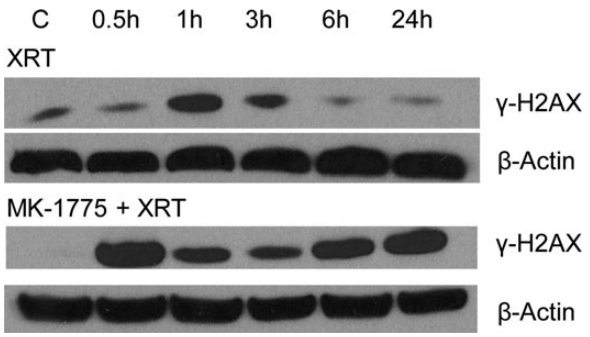

Fig. 5. Combination of MK-1775 and radiation leads to higher and more prolonged expression of dsDNA marker γ-H2AX. SF8628 DIPG xenograft cells treated with combination of radiation therapy (XRT, 2 Gy) and MK-1775 (200 nM), single modality only, or control. Western blots were performed at specified times after treatment to assess levels of γ-H2AX. Gamma-H2AX levels increase 1–3 h after radiation and return to baseline within 6 h, whereas in combination with MK-1775, elevated γ-H2AX levels are more pronounced and prolonged (at least 24 h after radiation).

In vivo Efficacy of MK-1775 in Combination With Radiation in Supratentorial and DIPG Pediatric Models

To address the in vivo efficacy of MK-1775 and radiation, we used 2 different orthotopic pediatric glioma models that both express

Wee1. For the first, genetically engineered mouse SF10776 cells carrying the *BRAF*^{V600E} mutation and modified for luciferase expression were injected supratentorially into athymic mice.[10] We chose SF10776 cells to model one of the most commonly found alterations in pediatric gliomas. Mice with intracranial SF10776 tumors and treated with MK-1775 and radiation showed significantly reduced tumor burden and longer survival than mice receiving single modality treatment (Fig. 6A). To test this combination therapy in a DIPG model, DIPG cells (SF8628) were injected directly into the brainstem, and mice were monitored for tumor bioluminescence. Mice with SF8628 DIPG treated with MK-1775 and radiation showed decreased tumor burden and increased survival compared with single modality or vehicle only treatment (Fig. 6B).

As observed in our in vitro studies, combination of MK-1775 and radiation increased γ-H2AX in orthotopic tumors treated in vivo (Fig. 7) to a greater extent than in tumors exposed to MK-1775 (Wilcoxon rank sum test, $P = .03$) or radiation alone (Wilcoxon rank sum test, $P = .03$). In addition, Ki-67, a marker of proliferation, was significantly reduced in the DIPG orthotopic tumors from mice treated with combination therapy compared with MK-1775 (Wilcoxon rank sum test, $P = .03$), radiation therapy (Wilcoxon rank sum test, $P = .03$), or control treated mice (Wilcoxon rank sum test, $P = .03$). Lastly, based on the underlying mechanism of action of MK-1775, we expected reduced expression of p-Cdc2 in xenografts from mice treated with MK-1775 or the combination of radiation and MK-1775. As shown in Fig. 7, expression of p-CDC2 was significantly reduced in the treatment groups that included MK-1775 compared with control or radiation alone ($P = .002$). Similar results were seen for SF10776 xenografts.

Discussion

In this investigation we demonstrated that Wee1 is significantly upregulated in pediatric gliomas and that treatment with the Wee1 inhibitor MK-1775 in combination with radiation increases the radiation cytotoxic effect and prolongs survival for mice with

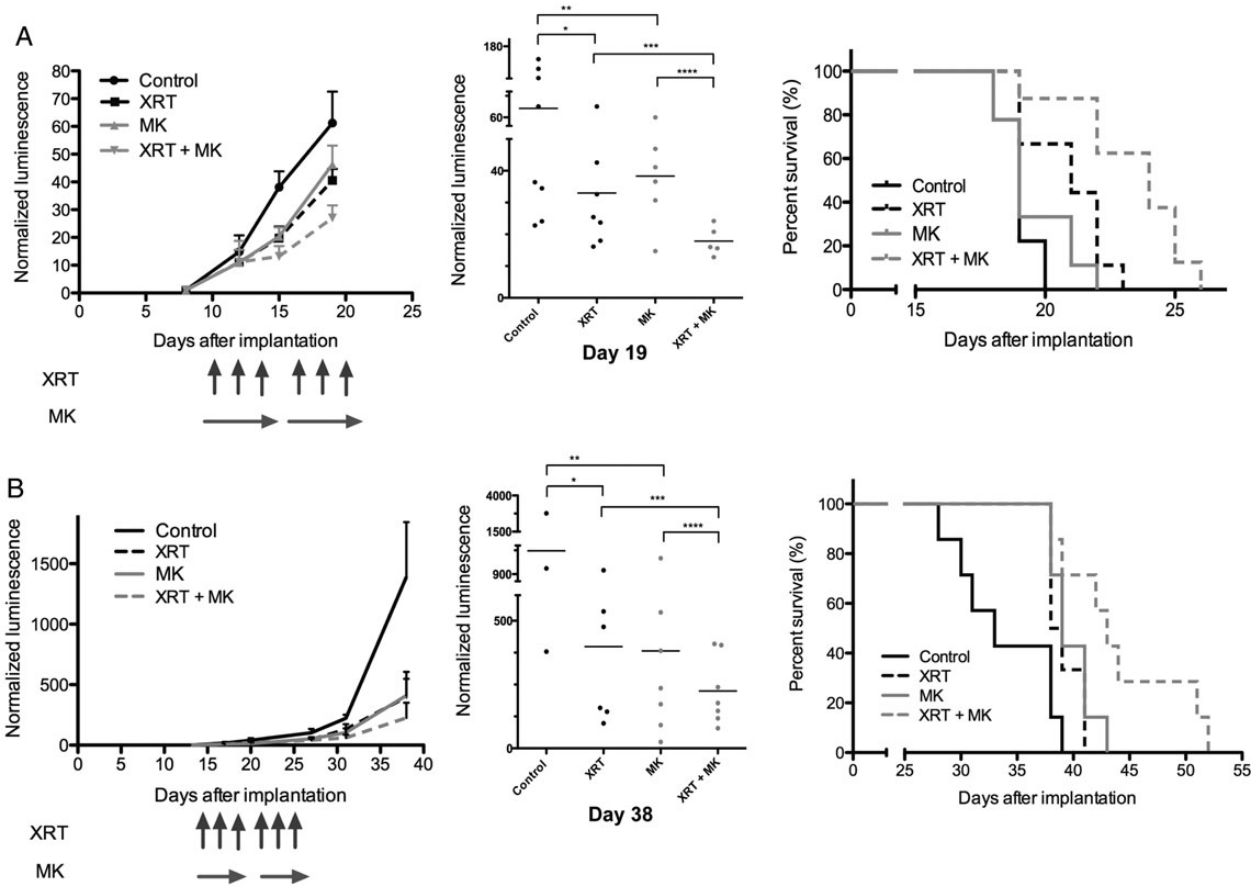

Fig. 6. Wee1 inhibitor MK-1775 augments radiation antitumor effect in vivo. (A) Intracerebral SF10776 HGG and (B) brainstem SF8628 DIPG xenografts treated with external beam radiation (XRT), MK (MK-1775), or XRT + MK-1775 beginning when tumors had entered log-phase growth as indicated by bioluminescence imaging tumor growth therapy response curves (left panels). Middle panels: Scatterplots of individual mice according to treatment cohort (day 19 for SF10776 [A] and day 38 for SF8638 [B]). *P* values for SF10776: control vs XRT, $^{*}P = .0411$; control vs MK-1775, $^{**}P = .0212$; XRT vs XRT + MK-1775, $^{***}P = .0137$; MK-1775 vs MK-1775 + XRT, $^{****}P = .0187$. *P* values for SF8628: control vs XRT, $^{*}P = .0199$; control vs MK-1775, $^{**}P = .0313$; XRT vs XRT + MK-1775, $^{***}P = .0424$; MK-1775 vs MK-1775 + XRT, $^{****}P = .0149$. Right panels: Kaplan–Meier survival plots; *P* values for SF10776: control vs XRT, $P = 0.0032$; XRT vs XRT + MK-1775, $P = .0061$; MK-1775 vs XRT + MK-1775, $P = .0009$. There is no significant difference in survival between control and MK-1775, $P = .235$. *P* values for SF8628: control vs XRT, $P = .0281$; control vs MK-1775, $P = .0077$; XRT vs XRT + MK-1775, $P = .0163$; MK-1775 vs MK-1775 + XRT, $P = .0467$.

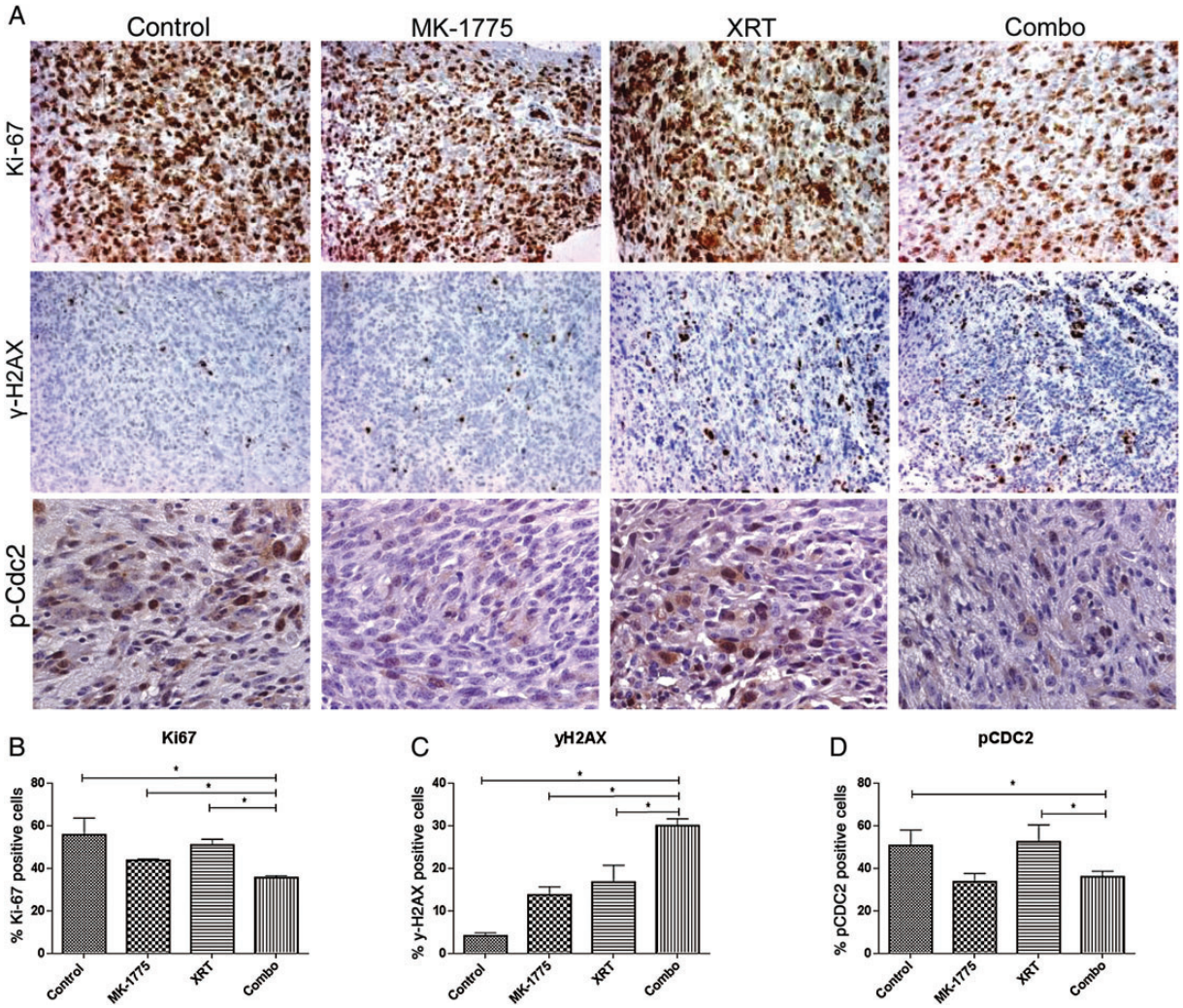

Fig. 7. IHC analyses of γ-H2AX and Ki-67 in human pediatric DIPG xenografts (SF8628). (A) Representative stains of intracranial xenografts resected 24 h after a 5-day treatment course of daily MK-1775 (60 mg/kg) for total of 5 days, with external beam radiation (XRT; 0.5 Gy) every other day (total dose 1.5 Gy), or MK-1775 (60 mg/kg × 5 days) + 0.5 Gy (every other day for total of 1.5 Gy), and control. Image-based quantification of (B) Ki-67, (C) γ-H2AX, and (D) p-Cdc2. Percent positive tumor cells were determined in at least five 20× images per tumor, and averaged. Bars represent SE. Indicated differences between groups as indicated by Kruskal–Wallis test, followed by Wilcoxon rank sum test pairwise comparisons. Ki-67: combination therapy vs control $P = .03$, vs XRT $P = .03$, vs MK-1775, $P = .03$. Gamma-H2AX: combination therapy vs control $P = .03$, vs XRT $P = .03$, vs MK-1775 $P = .03$. p-Cdc2: combination therapy vs control and XRT $P = .002$, vs MK-1775, $P = .06$. Asterisk indicates statistically significant differences.

engrafted, orthotopic gliomas. Two distinct engraftment models were used: one involving tumor cells from a genetically engineered mouse with *BRAF*^{V600E} mutation, and the other involving human tumor cells propagated from a patient's DIPG. Similar results have been recently reported in association with the use of an adult glioma for animal modeling of DIPG.[16] To our knowledge, the current report is the first using pediatric HGG models to assess the effects of Wee1 inhibition in combination with radiation. Importantly, MK-1775 is the only specific Wee1 inhibitor that has entered clinical trials and has a favorable side effect profile. Our results therefore support combination therapy of MK-1775 and radiation as a promising new treatment strategy for children with HGGs including DIPGs.

The combination of radiation and a Wee1 inhibitor represents one of the first treatment concepts to capitalize on a specific molecular characteristic of pediatric malignant gliomas, namely their high level of Wee1 expression. Our results show that Wee1 expression positively correlates with glioma grade, with highest expression found in DIPG samples, consistent with a published gene expression dataset for 27 DIPGs, in which we found that Wee1 was significantly upregulated in DIPGs compared with normal brain.[13] Recently, others have reported significantly elevated Wee1 expression in DIPGs compared with low-grade glioma and normal brain samples, consistent with our findings.[16]

Prior studies have shown that Wee1 expression levels predict response to Wee1 inhibition.[7] Consistent with this, the SF8628 DIPG xenograft we examined, which showed the highest level of Wee1 expression of our entire tumor cohort, was more responsive to radiation + MK-1775 combination therapy than to radiation alone. Moreover, all tested HGG cell lines were sensitive to MK-1775 and

radiation, irrespective of p53 status, suggesting that p53 mutation is not essential for cell sensitivity to Wee1 inhibition, as previously reported for adult GBM[7] and sarcomas.[8] In contrast, others have shown that certain types of cancer may be dependent on p53 mutation for response to Wee1 inhibition.[17,18] Of note, our DER values were very similar in the various cell lines in vitro, and therefore we cannot draw any firm conclusions regarding association between Wee1 expression and response to MK-1775.

With respect to mechanism of action, we confirm that radiation arrests pediatric glioma cells in G_2 and that MK-1775 promotes abrogation of this cell cycle checkpoint. MK-1775–treated cells are therefore less able to repair radiation-induced DNA damage prior to entering mitosis, as demonstrated by analysis of γ-H2AX levels (Figs. 5 and 7), resulting in increased cell death.[7] However, our data are consistent with MK-1775 increasing dsDNA breaks not only by abrogation of G_2 arrest but also due to direct effects on the DNA repair machinery. DNA repair is highly regulated and often specific to the type of incurred DNA damage. Nonhomologous end-joining and homologous recombination are activated by radiation-induced dsDNA breaks and involve numerous proteins, including Ku heterodimer (Ku70/Ku80), DNA protein kinases, ligase IV, X-ray repair cross-complementing protein 4 (XRCC4) and XRCC4-like factor, Artemis and DNA polymerases for nonhomologous end-joining, and Rad51 for homologous recombination.[19] Precedence exists in the literature regarding direct involvement of cell cycle regulators in the DNA repair machinery, including ataxia telangiectasia mutated kinase and Chk1.[20,21] Further investigations are needed to clarify whether (1) abrogation of cell cycle arrest is the main mechanism by which Wee1 inhibition enhances the cytotoxic effects of radiation or (2) a possible direct role for Wee1 in the DNA repair machinery contributes to its cooperative antitumor effects with radiation.

Conclusions

Wee1 is overexpressed in pediatric gliomas, and Wee1 expression levels positively correlate with increasing glioma grade. MK-1775 promotes abrogation of the radiation-induced G_2 arrest, increases and prolongs tumor γ-H2AX, and thereby radiosensitizes pediatric HGGs. MK-1775 in combination with radiation extended survival compared with single modality arms in 2 independent orthotopic pediatric glioma models, one a supratentorial HGG and the second a newly established DIPG xenograft model. Results of this preclinical study provide a strong rationale for a phase 1 trial of the combination of MK-1775 and radiation in children newly diagnosed with DIPG.

Supplementary Material

Supplementary material is available online at *Neuro-Oncology* (http://neuro-oncology.oxfordjournals.org/).

Funding

This research was supported in part by a National Institute of Neurological Disorders and Stroke grant (K12NS001692 to S.M.), the National Center for Advancing Translational Sciences, National Institutes of Health (NIH), through UCSF-CTSI grant KL2TR000143 (S.M.), NIH Brain Tumor SPORE grant P50 CA097257 (S.M., D.A.H-K., M.D.P., M.S.B.), The V Foundation (S.M., D.A.H-K.), the Matthew Larson Foundation (S.M.), and the A. Frank Campini Foundation (S.M.).

Acknowledgments

Dr Rowitch (Department of Pediatrics, UCSF) generously provided SF10776 cells. We would like to thank Cynthia Cowdrey for assistance with the IHC analysis.

Conflict of interest statement. None declared.

References

1. Hargrave D, Bartels U, Bouffet E. Diffuse brainstem glioma in children: critical review of clinical trials. *Lancet Oncol*. 2006;7(3):241–248.
2. Nicolaides TP, Li H, Solomon DA, et al. Targeted therapy for BRAFV600E malignant astrocytoma. *Clin Cancer Res*. 2011;17(24):7595–7604.
3. Zarghooni M, Bartels U, Lee E, et al. Whole-genome profiling of pediatric diffuse intrinsic pontine gliomas highlights platelet-derived growth factor receptor alpha and poly (ADP-ribose) polymerase as potential therapeutic targets. *J Clin Oncol*. 2010;28(8):1337–1344.
4. Wu G, Broniscer A, McEachron TA, et al. Somatic histone H3 alterations in pediatric diffuse intrinsic pontine gliomas and non-brainstem glioblastomas. *Nat Genet*. 2012;44(3):251–253.
5. Khuong-Quang DA, Buczkowicz P, Rakopoulos P, et al. K27M mutation in histone H3.3 defines clinically and biologically distinct subgroups of pediatric diffuse intrinsic pontine gliomas. *Acta Neuropathol*. 2012;124(3):439–447.
6. Paugh BS, Qu C, Jones C, et al. Integrated molecular genetic profiling of pediatric high-grade gliomas reveals key differences with the adult disease. *J Clin Oncol*. 2010;28(18):3061–3068.
7. Mir SE, De Witt Hamer PC, Krawczyk PM, et al. In silico analysis of kinase expression identifies WEE1 as a gatekeeper against mitotic catastrophe in glioblastoma. *Cancer Cell*. 2010;18(3):244–257.
8. Kreahling JM, Gemmer JY, Reed D, Letson D, Bui M, Altiok S. MK1775, a selective Wee1 inhibitor, shows single-agent antitumor activity against sarcoma cells. *Mol Cancer Ther*. 2012;11(1):174–182.
9. Sarkaria JN, Yang L, Grogan PT, et al. Identification of molecular characteristics correlated with glioblastoma sensitivity to EGFR kinase inhibition through use of an intracranial xenograft test panel. *Mol Cancer Ther*. 2007;6(3):1167–1174.
10. Huillard E, Hashizume R, Phillips JJ, et al. Cooperative interactions of BRAFV600E kinase and CDKN2A locus deficiency in pediatric malignant astrocytoma as a basis for rational therapy. *Proc Natl Acad Sci U S A*. 2012;109(22):8710–8715.
11. Franken NA, Rodermond HM, Stap J, Haveman J, van Bree C. Clonogenic assay of cells in vitro. *Nat Protoc*. 2006;1(5):2315–2319.
12. Bolstad BM, Irizarry RA, Astrand M, Speed TP. A comparison of normalization methods for high density oligonucleotide array data based on variance and bias. *Bioinformatics*. 2003;19(2):185–193.
13. Paugh BS, Broniscer A, Qu C, et al. Genome-wide analyses identify recurrent amplifications of receptor tyrosine kinases and cell-cycle regulatory genes in diffuse intrinsic pontine glioma. *J Clin Oncol*. 2011;29(30):3999–4006.

14. Hashizume R, Smirnov I, Liu S, et al. Characterization of a diffuse intrinsic pontine glioma cell line: implications for future investigations and treatment. *J Neurooncol*. 2012;110(3):305–313.
15. Mueller S, Yang X, Sottero TL, et al. Cooperation of the HDAC inhibitor vorinostat and radiation in metastatic neuroblastoma: efficacy and underlying mechanisms. *Cancer Lett*. 2011;306(2):223–229.
16. Caretti V, Hiddingh L, Lagerweij T, et al. WEE1 kinase inhibition enhances the radiation response of diffuse intrinsic pontine gliomas. *Mol Cancer Ther*. 2013;12(2):141–150.
17. Hirai H, Iwasawa Y, Okada M, et al. Small-molecule inhibition of Wee1 kinase by MK-1775 selectively sensitizes p53-deficient tumor cells to DNA-damaging agents. *Mol Cancer Ther*. 2009;8(11):2992–3000.
18. Krajewska M, Heijink AM, Bisselink YJ, et al. Forced activation of Cdk1 via wee1 inhibition impairs homologous recombination. *Oncogene*. 2013; 32(24):3001–3008.
19. Branzei D, Foiani M. Regulation of DNA repair throughout the cell cycle. *Nat Rev Mol Cell Biol*. 2008;9(4):297–308.
20. Goodarzi AA, Noon AT, Deckbar D, et al. ATM signaling facilitates repair of DNA double-strand breaks associated with heterochromatin. *Mol Cell*. 2008;31(2):167–177.
21. Morgan MA, Parsels LA, Zhao L, et al. Mechanism of radiosensitization by the Chk1/2 inhibitor AZD7762 involves abrogation of the G2 checkpoint and inhibition of homologous recombinational DNA repair. *Cancer Res*. 2011;70(12):4972–4981.